

Emission from the Galaxy NGC 1275 at High and Very High Energies and Its Origin

V. G. Sinitsyna and V. Yu. Sinitsyna*

*Lebedev Physical Institute, Russian Academy of Sciences,
Leninskii pr. 53, Moscow, 119991 Russia*

(Dated: Received April 12, 2013; in final form, October 13, 2013)

Abstract – The Seyfert galaxy NGC 1275 is the central, dominant galaxy in the Perseus cluster of galaxies. NGC1275 is known as a powerful source of radio and X-ray emission. The well-known extragalactic object NGC 1275 has been observed by the SHALON high-altitude mirror Cherenkov telescopes within the framework of long-term studies of metagalactic gamma-ray sources. In 1996, the SHALON observations revealed a new metagalactic source of very high energy gamma-ray emission coincident in its coordinates with the galaxy NGC 1275. Having analyzed the SHALON data, we have determined such characteristics of NGC 1275 as the spectral energy distributions and images at energies >800 GeV for the first time. The results obtained at high and very high energies are needed for understanding the emission generation processes in an entire wide energy range.

Keywords: Seyfert galaxy, NGC 1275, Perseus cluster of galaxies

INTRODUCTION

The cluster of galaxies in Perseus is one of the best-studied clusters owing to its relative proximity (its distance 100 Mpc or redshift $z = 0.0179$) and brightness. Clusters of galaxies have long been considered as possible candidates for the sources of TeV gamma-rays emitted by protons and electrons accelerated at large-scale shocks or by a galactic wind or active galactic nuclei (Dennison 1980; Houston et al. 1984; Colafrancesco and Blasi 1998; Sarazin 1999; Miniati et al. 2001; Timokhin et al. 2004; Colafrancesco and Marchegiani 2009). The dominant galaxy in the Perseus cluster is NGC 1275.

NGC 1275

The galaxy NGC 1275 has been classified in various ways, for example, as a Seyfert 1.5 galaxy, because broad emission lines were detected in its spectrum at optical wavelengths (Veron-Cetty and Veron 1998). However, within the unified model of active galactic nuclei (AGNs) (Fanaroff and Riley 1974; Urry and Padovani 1995), it also belongs to the main class of BL Lacertae objects owing to its large and fast flux variability and polarization (Angel and Stockman 1980). It should be noted

that there is evidence that the mentioned AGN unification scheme can be even simplified (Kharb et al. 2010).

NGC 1275 is a powerful source of radio and X-ray emission. In the radio band, the object found in NGC 1275, also known as Perseus A and 3C 84, has a powerful and compact core that has been well studied with VLBI (Vermeulen et al. 1994; Taylor and Vermeulen 1996; Asada et al. 2006). NGC 1275 is extremely bright in the radio band and was classified as an FR I radio galaxy; it has a prominent structure that consists of a compact central source and an extended jet (Vermeulen et al. 1994; Asada et al. 2009). Having a supermassive black hole (with a mass of $3.4 \times 10^8 M_\odot$) at its center (Wilman et al. 2005), NGC 1275 also exhibits jet precession, which can be interpreted as a possible manifestation of the fact that NGC 1275 is the result of a merger between two galaxies (Liu and Chen 2007). The radio emission extends to great distances and shows a clear interaction with the gas inside the Perseus cluster of galaxies. ROSAT (Böhringer et al. 1993) and, subsequently, Chandra (Fabian et al. 2006) observations revealed cavities in the gas located inside the cluster, whose presence suggests that the jets from 3C 84 sweep up numerous "bubbles" in the atmosphere of the Perseus cluster (Fig. 1).

The galaxy NGC 1275 surrounded by extended filamentary structures historically aroused great interest owing to both its position at the center of the Perseus cluster and its possible "feedback" role (Gallagher 2009). Evidence for the "feedback" role of NGC 1275 can be obtained from ROSAT and Chandra observations, which

*Electronic address: sinits@sci.lebedev.ru

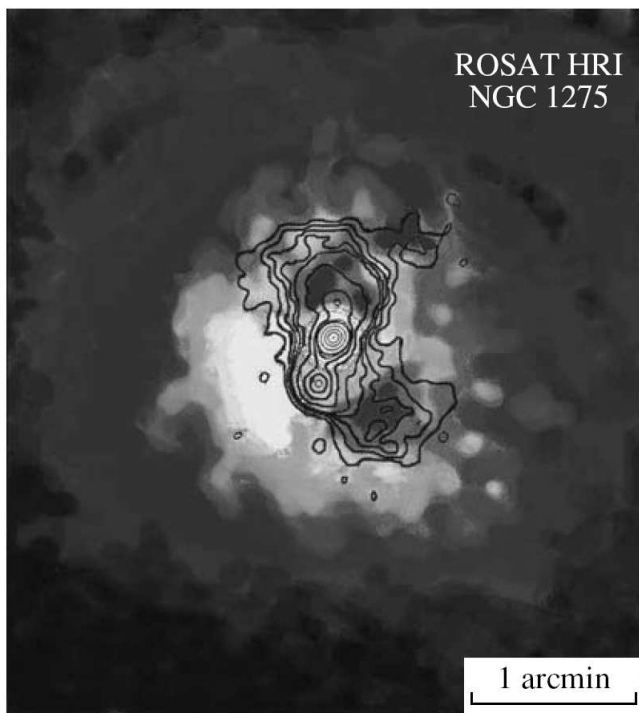


FIG. 1: ROSAT X-ray (0.1 - 2.4 keV) image of NGC 1275 (Böhringer et al. 1993). The contours represent the sources radio structure from VLA radio observations. The radio and X-ray emission maxima coincide with the active galactic nucleus NGC 1275, while the X-ray emission disappears almost completely near the bright areas of the radio components.

reveal shells of hot gas and cavities that spatially coincide with the radio structures (Fig. 1) extending from the central, active part of the AGN. NGC 1275 also arouses interest owing to its close proximity to the Earth at redshift $z = 0.0179$ (Strauss et al. 1992), making it possible to study the physics of relativistic jets.

Upper limits on the gamma-ray emission from the Perseus cluster of galaxies and its central galaxy NGC 1275 were obtained in various experiments onboard satellites. The first observations were performed with the COS-B telescope from 1975 to 1979 (Strong et al. 1982) and then with the EGRET facility in 1995 (Thompson et al. 1995).

At very high energies, upper limits were obtained in different years in ground-based experiments, such as the large-area scintillation Tibet Array at $E > 3$ TeV (1999) (Amenomori 1999), and at the Cherenkov telescopes Whipple (2006) (Perkins et al. 2006) at energies > 400 GeV, MAGIC (2009) (Aléksic et al. 2010) at $E > 100$ GeV, and Veritas (2009) (Acciari et al. 2009) at $E > 188$ GeV. Recently, NGC 1275 was recorded at high energies, 100 MeV - 300 GeV, by the Fermi LAT satellite telescope (Abdo et al. 2009). To understand the emission generation processes in the entire energy range, the spectral energy distribution should be extended up to very high energies.

In this paper, we describe both the results of fifteen-year-long studies for the AGN NGC 1275 obtained at very high energies with the SHALON mirror Cherenkov telescope and the experimental approach to searching for the gamma-ray emission mechanisms in clusters of galaxies and AGNs located in the cluster atmosphere.

THE SHALON MIRROR CHERENKOV TELESCOPES

The SHALON mirror gamma-ray telescopes of the Lebedev Physical Institute, the Russian Academy of Sciences, with which the data presented here were obtained are the only operating gamma-ray telescopes in the Russian Federation and one of the five telescopic facilities in the world that are currently performing systematic observations of local gamma-ray sources at TeV energies. Methodical experiments and observations at the first SHALON mirror Cherenkov telescope were begun twenty years ago. The SHALON experiment and its main characteristics are described in Sinitsyna (1995, 1996, 1997, 2000, 2006), Sinitsyna et al. (1998, 2003, 2007, 2009), Nikolsky and Sinitsyna (1989, 2004), and V.G. Sinitsyna and V.Yu. Sinitsyna (2011a, 2011b). The telescopes parameters, the observing technique, and the selection criteria of gamma-ray showers from background cosmic-ray showers are also described in Nikolsky and Sinitsyna (1989), Sinitsyna (1995, 1996), and V.G. Sinitsyna and V.Yu. Sinitsyna (2011a, 2011b).

The SHALON ALATOO mirror Cherenkov telescope system (Fig. 2) is designed to observe gamma rays from local sources in the energy range from 800 GeV to 100 TeV. The SHALON gamma-ray telescopes are located at an altitude of 3340 m above sea level each of which has a composite mirror with an area of 11.2 m². The detector array consisting of 144 FEU-85 photomultiplier tubes assembled into a square array and mounted at the mirror focus has characteristics sufficient to record information about the shower structure in the energy range under consideration. The detector has the largest field of view in the world, $> 8^\circ$. This allows one to monitor the background from charged cosmic-ray particles and the atmospheric transparency continuously during observations and expands the area of observation and, hence, the efficiency of observations (Nikolsky and Sinitsyna 1989; Sinitsyna 1995, 1996). The technique for simultaneously obtaining information about the cosmic-ray background and the showers initiated by gamma rays is unique and has been applied in the SHALON experiment from the very beginning of its operation (Nikolsky and Sinitsyna 1989; Sinitsyna 1995, 1996). This technique serves to increase the useful source tracking time and, what is particularly important, such source and background observation conditions as the thickness and state of the atmosphere remain the same. This method is inaccessible to other gamma-ray astronomical experiments, because the telescopes used in the world have a smaller field of

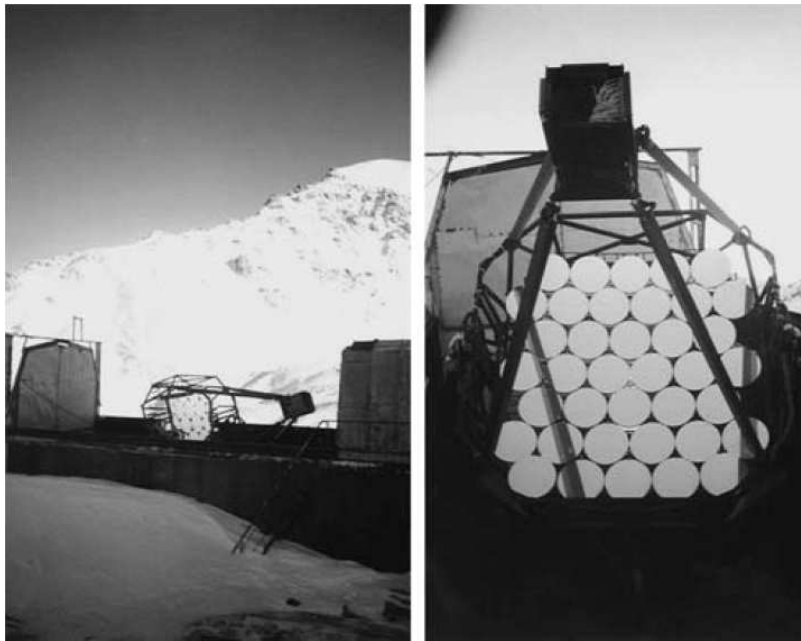


FIG. 2: SHALON-1 mirror Cherenkov telescope in the observatory.

view. In addition, the wide field of view allows recording the off-center showers arriving at distances of more than 30m from the telescope axis completely and almost without any distortions; they account for more 90% of all the showers recorded by the telescope. During a primary analysis, the primary particle arrival direction is determined with an accuracy up to $\lesssim 0.1^\circ$. The subsequent analysis specially developed for the SHALON telescopes and based on Tikhonov's regularization method (Tikhonov and Arsenin 1979; Goncharsky et al. 1985) improves the accuracy to a value of less than 0.01° .

The main difficulty in detecting and investigating very high energy gamma-ray sources is the presence of a significant (a factor of 1000 larger) background of cosmic rays producing the Cherenkov flashes in the Earth's atmosphere that are hard to distinguish from the flashes produced by gamma rays. Therefore, the determination of the criteria for selecting gamma-ray showers from background cosmic-ray showers (Sinitsyna 1996; V.G. Sinitsyna and V.Yu. Sinitsyna 2011b) is an important stage of gamma-ray astronomical experiments.

The distributions of the shower image parameters used in the SHALON experiment as a selection criteria optimized from the Monte Carlo simulations are presented in Figs. 3 - 5 below (Sinitsyna 1996). The simulation correctness is confirmed by the distributions of shower image parameters both for background of cosmic rays and for gamma-rays from the point sources obtained experimentally in observations (Sinitsyna 2003; V.G. Sinitsyna and V.Yu. Sinitsyna 2011b).

The Cherenkov radiation from an extensive air shower (EAS) falls on the mirrors and, being reflected from

them, illuminates some of the photomultiplier tubes in the detector array (V.G. Sinitsyna and V.Yu. Sinitsyna 2011b). The image of the Cherenkov light from a shower in the detector plane is generally an elliptical light spot with a central peak. Analyzing the angular and lateral distributions of the shower Cherenkov light is of great interest for the selection of showers of primary gamma-rays. The so-called Hillas parameters (Hillas 1985) : α , *Length*, *Width*, and *Distance* are used for these purposes in gamma-ray astronomy and optimized for each experiment individually. The distributions of α (degrees) and *Distance* (pixels) for gamma-ray showers and background showers in the SHALON experiment are presented in Fig. 3. About 72% of the background events can be rejected by applying the constraint $\alpha < 20$. Taking *Distance* < 3.5 pixels as a criterion, we remove $\sim 50\%$ of the background cosmic-ray showers.

Analysis of the distribution of *Length* and *Width* shower image parameters showed that the mean values of these parameters for gamma-ray and proton showers are, in principle, identical and, hence, they cannot serve as a selection criterion. However, the mean ratio *Length/Width* is different for different types of showers and is stable against a change in energy. Taking *Length/Width* > 1.6 as a criterion, we thus reject $\sim 49\%$ of the background showers, leaving the number of gamma-ray showers intact (see Fig. 4).

Moreover, in addition to the standard criteria, it turned out to be appropriate to construct one more characteristic of the light spot which is based on the difference between the characteristics of cascades of primary particles of a different nature. As a result, selection crite-

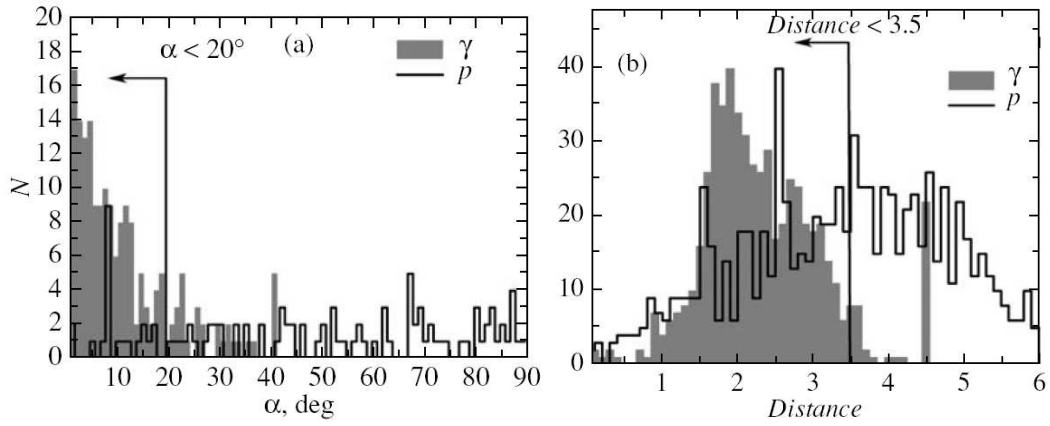


FIG. 3: Distributions of the parameters α (a) and $Distance$ (b) for gamma-ray showers and background showers (black contour).

ria of the gamma-ray showers from the background ones ($Int0$, $Int1$) that are based on the difference between their spatial characteristics were specially developed for the SHALON gamma-ray telescope. For these purpose we use the difference between their spatial characteristics, i.e., on the difference between the characteristics of EASs of a different nature (Sinitsyna 1995, 1996; V.G. Sinitsyna and V.Yu. Sinitsyna 2011b), if comparing the photon fluxes within a small angle of less than 1° around the cascade axis with the flux within large angles of more than 2° (Nikolsky and Sinitsyna 1987) were specially developed for the SHALON gamma-ray telescope. As a result, the parameters with which the gamma-ray showers could be selected from the entire set of available experimental light images were obtained. The pixel with the maximum intensity (photoelectron density) $Intmax$ is chosen in the array with a light image. Then, eight

pixels surrounding the maximum one are taken and the photoelectron intensities are summed in them. The sum is designated as $Inteig$. The sum of the photoelectron intensities in the remaining pixels (except for the nine above-mentioned ones) is designated as $Intsur$ and the following ratios are constructed: $Int0 = Intmax/Inteig$ and $Int1 = Intmax/Intsur$. The constraints on these parameters for an efficient selection of gamma-ray showers from cosmic-ray showers were derived from the distributions of $Int0$ and $Int1$ (Fig. 5): $Int0 > 0.6$ and $Int1 > 0.8$. When the parameters $Int0$ and $Int1$ are applied, 92 and 88% of the background showers, respectively, are rejected.

Analysis of the distributions showed that the following selection criteria applied in the SHALON experiment ($\alpha < 20^\circ$, $Length/Width > 1.6$, $Int0 > 0.6$, $Int1 > 0.8$, $Distance < 3.5$ pixels) reject 99.92% of the background, while, according to our estimations, the loss of gamma rays does not exceed 35%, which is taken into account in the subsequent analysis, but the contribution of the background showers to the selected gamma-ray ones being no more than 10%.

The primary particle arrival direction and further construction of the image are performed within a two-step procedure.

At the first step, the coordinates of the shower source position on the light receiver plane for each of the showers selected according to the described criteria are found. The shower image in the array is characterized by an ellipse with the major axis that is the projection of the shower axis onto the lightreceiver plane. The gamma-ray shower source is on the extension of the major axis of such an ellipse from the side of the shower maximum corresponding to the cascade beginning. The distance from the centroid of the shower image to the sources position, D , depends on the distance at which the shower arrived and, as a result, on the shower elongation by the parameter $Length/Width$. This dependence can be written as $D = B \times [1 - (Length/Width)^{-1}]$. The optimal proportionality coefficient $B = 5.1$ was chosen in such a

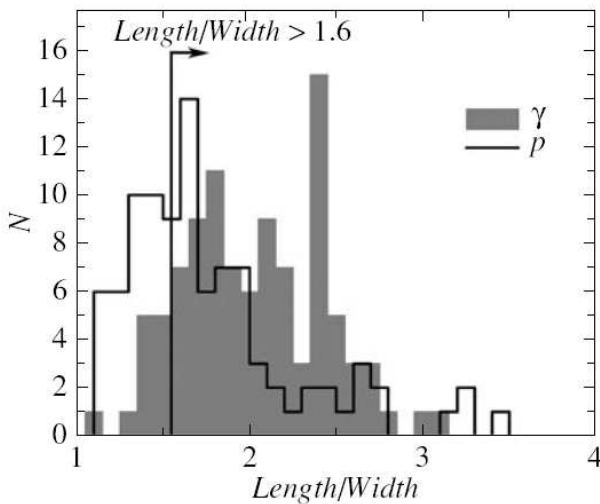


FIG. 4: Distribution of the parameter $Length/Width$ for gamma-ray showers and background showers (black contour).

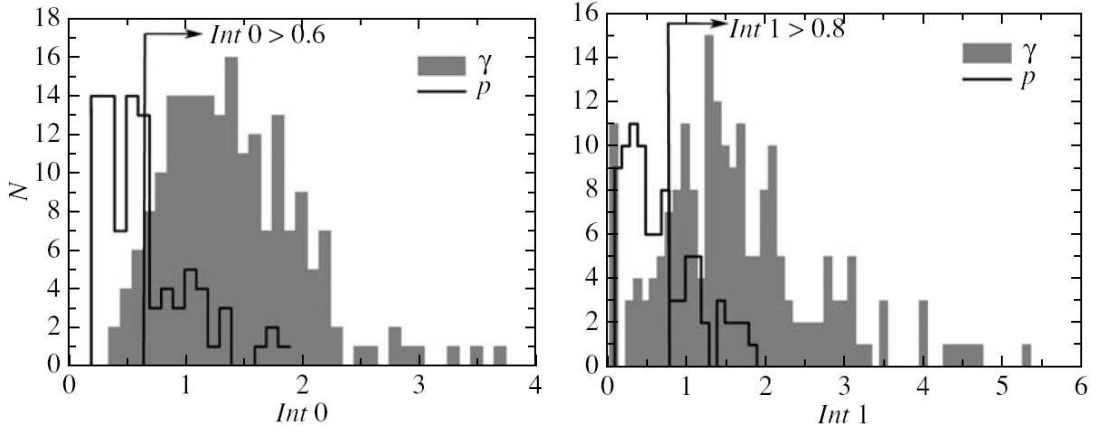


FIG. 5: Distributions of the parameters $Int0$ (left) and $Int1$ (right) for gamma-ray showers and background showers (black contour).

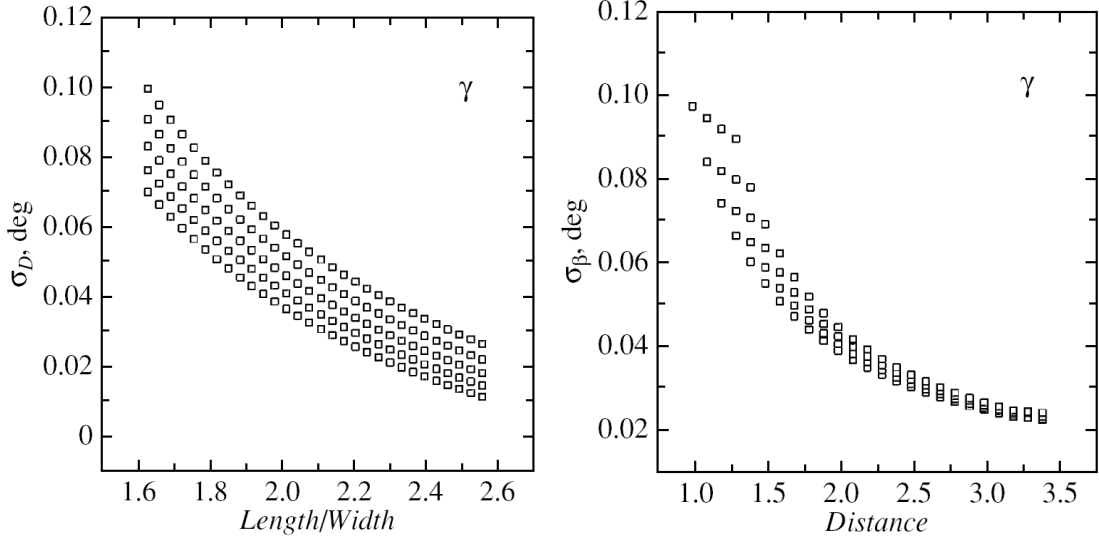


FIG. 6: Accuracies of the determination of the coordinates D (left) and β (right) for the point of the shower source on the light receiver plane in the shower energy range 1 - 100 TeV.

way that the distribution of shower arrival directions in angles was minimal in width and centered at the sources position on the array.

The second coordinate β is the inclination of the major axis of the ellipse and can be defined via the parameter Distance. The accuracies of the determination of each of these coordinates are presented in Fig. 6 and are $0.07^\circ \pm 0.01^\circ$ and $0.045^\circ \pm 0.01^\circ$, respectively, for the mean values of $Length/Width$ and $Distance$ (Figs. 3 and 4).

At the second step, an additional analysis of the gamma-ray shower source coordinates obtained at the first step is performed and the gamma-ray intensity distribution in the source is found. Finding the gamma-ray intensity distribution in the source $I(r)$ is reduced to solving a Fredholm integral equation of the first kind: $F(z) = \int K(r, s)I(s)ds$ where $K(r, s)$ is the kernel func-

tion defined as a Gaussian point spread function with the full widths half magnitude σ_D and σ_β determined at the first step. Then, we refine the observed distribution from Fig. 7a by solving an integral equation (Goncharskii et al. 1985) under the assumption that the solution is a smooth nonnegative upper-bounded function, as the sources angular sizes were limited, and the solution was definitely within the region determined at the first step. Figure 7b presents the corrected gamma-ray intensity distribution $I(r)$, where $r(SE)$ is the distance to the southeast from the nucleus of NGC 1275 in degrees. As a result of the second step, the accuracy of the determination of the coordinates of the gamma-ray shower source increases by a factor of ~ 10 compared to the first step and it becomes possible to find the gamma-ray intensity distribution in the source and its surroundings.

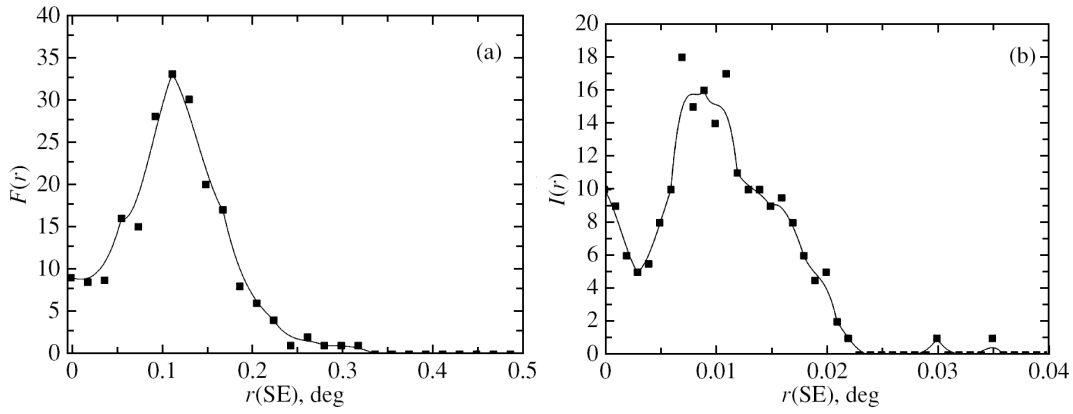


FIG. 7: (a) Gamma-ray intensity distribution obtained at the first step; (b) gamma-ray intensity distribution in the source after the correction at the second step.

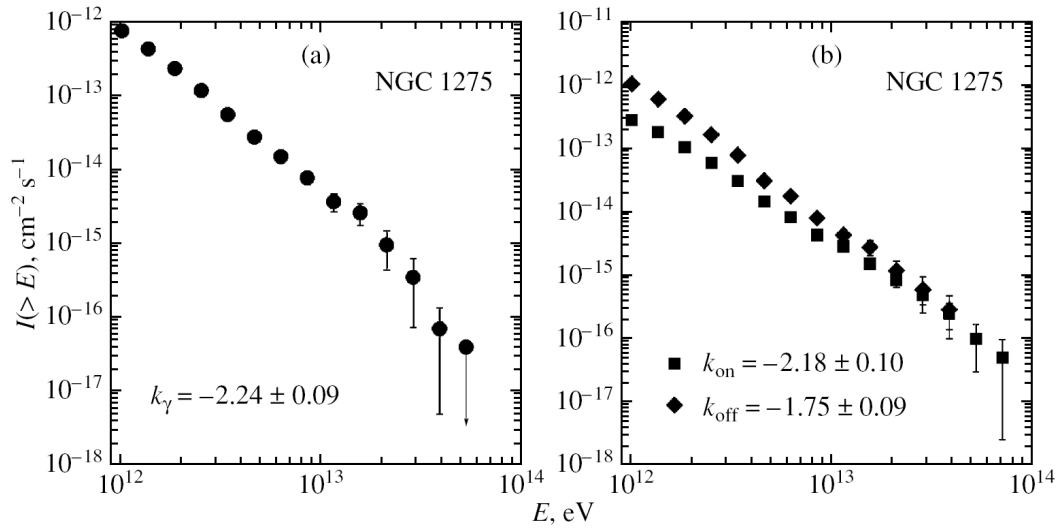


FIG. 8: (a) Gamma-ray spectrum of NGC1275 with a power-law index $k_\gamma = -2.24 \pm 0.09$; (b) the spectrum of the events from NGC 1275 that passed the selection criteria without subtracting the background with $k_{on} = -2.18 \pm 0.10$ and the spectrum of the background events observed simultaneously with the source with $k_{off} = -1.75 \pm 0.09$.

NGC 1275 AT VERY HIGH ENERGIES

Metagalactic sources of very high energy gamma-rays have been searched for in the SHALON experiment from the very beginning of its operation (Sinitsyna 1995, 1996). In 1996, the observations with the SHALON mirror Cherenkov telescope revealed a new metagalactic source of gamma-ray emission at very high energies $E > 800$ GeV (Sinitsyna et al. 1998; Sinitsyna 2000) (Figs. 8 and 9). The position of emission source detected in our experiment coincides in its coordinates with the Seyfert galaxy NGC 1275 (Sinitsyna 1997, 2000, 2006; Sinitsyna et al. 1998, 2003, 2007, 2009; Nikolsky and Sinitsyna 2004). NGC 1275 was observed by the SHALON telescope for 271.2 h in different years (from 1996 to 2012) during the clear moonless nights at zenith angles from

3° to 33° . The observations were performed using the standard (for SHALON) technique of obtaining information about the cosmic-ray background and gamma-ray-initiated showers in the same observing session (Sinitsyna 1996; V.G. Sinitsyna and V.Yu. Sinitsyna 2011a, 2011b). Gamma-ray emission from NGC 1275 was detected by the SHALON telescope at energies above 800 GeV at the 31.4σ confidence level determined according to Li and Ma (1983). The average integral flux at energies above 800 GeV for NGC 1275 is $I_{NGC1275} = (7.8 \pm 0.5) \times 10^{-13} \text{ cm}^{-2} \text{ s}^{-1}$ (Fig. 8).

Figure 8b presents the spectra of the *on* and *off* events needed to extract the gamma-ray spectrum from NGC 1275. The gamma-ray spectrum of NGC 1275 is obtained by subtracting the spectrum of the background events recorded simultaneously with the source's observations,

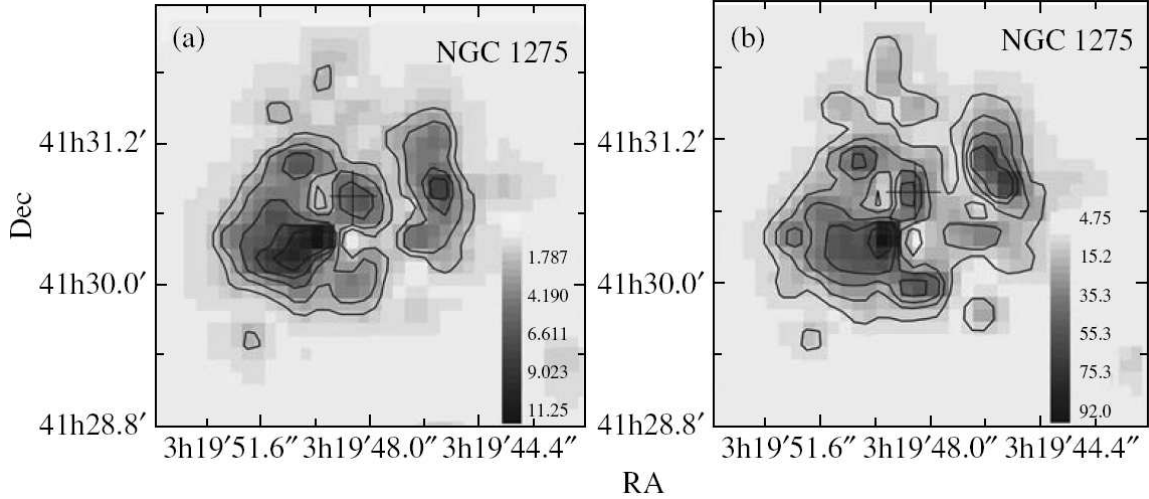


FIG. 9: (a) SHALON image of the gamma-ray source NGC 1275 at energies >0.8 TeV; (b) the energy image of NGC 1275.

$I_{off} \propto E^{k_{off}}$, from the spectrum of the events arrived from the source position, $I_{on} \propto E^{k_{on}}$. The integral spectrum of the *off* events was constructed from statistics larger than that of *on* events by a factor of 4, because it is an averaging over the background taken from four regions far away from the source but equal in angular size to the source's region. The gamma-ray energy spectrum in the observed energy range above 0.8 TeV is well described by a power law $F(E_0 > 0.8 \text{ TeV}) \propto E^{k_\gamma}$, where $k_\gamma = -2.24 \pm 0.09$ (see Fig. 8a; see the Appendix).

Figure 9 presents the sources image at TeV energies and its energy image by SHALON experiment. The color scale in Fig. 9a on the left is in units of the excess above the minimum detected signal for the energy image (in TeV).

Possible correlations between the emission regions of TeV gamma rays and low-energy (radio and X-ray) photons should be established to elucidate the mechanisms of the generation of very high energy emission in the source and to test the models describing them. Figure 1 shows a ROSAT X-ray image of NGC 1275 (black-and-white scale); the contours represent the sources radio structure from VLA radio observations. The radio and X-ray emission maxima coincide with the AGN NGC 1275. At the same time, the X-ray emission disappears almost completely near the bright areas of the radio components located in the north and the south symmetrically relative to the core (Böhringer et al. 1993). We also combined the SHALON-1 (0.8 – 40 TeV) and Chandra (1.5 – 3.5 keV X-ray) images. Figure 10 (black-and-white scale) presents a Chandra X-ray (1.5 – 3.5 keV) image for the central part of the Perseus cluster centered on NGC 1275 with a size of ~ 5.5 arcmin (Fabian et al. 2000). In the X-ray energy range, the core of the Perseus cluster, on the whole, appears as a clear circularly symmetric structure with a distinct maximum on NGC 1275.

The clearly seen dimming in X-ray flux, along with

the dip NW of the center, known from the 1979 Einstein observations (Fabian et al. 1981), correlates with the components of the extended double radio structure 3C 84 (Fig. 1). These dips are surrounded by bright (at energies 1.5 – 3.5 keV) arc regions from the north and the south. The simplest interpretation is that the intense emission from these rims comes from the shells surrounding the radio lobes (Fabian et al. 2000). A bright emission spot is also observed to the east.

The emission regions of very high energy gamma rays observed by SHALON from NGC 1275 have a structure similar to that described above (see Fabian et al. 2000) and well correlates with the photon emission regions in the energy range 1.5 – 3.5 keV (Fig. 10). A correlation of the emission with energies 0.8 – 40 TeV (Sinitsyna et al. 2003, 2007, 2009) and the X-ray emission in the range 0.3 – 7 keV (Fabian et al. 2000) was also found. Thus, the TeV gamma-ray emission recorded by SHALON from NGC 1275 has an extended structure with a distinct core centered at the sources position.

To analyze the emission related to this core, we additionally identified the emission component corresponding to the central region of NGC 1275 with a size of $32''$. The emission from the central region of NGC 1275 was detected at energies above 0.8 TeV at a 13.5σ confidence level determined by the Li&Ma method (Li and Ma 1983) with a average integral flux $I(> 800 \text{ GeV}) = (3.26 \pm 0.30) \times 10^{-13} \text{ cm}^{-2} \text{ s}^{-1}$. The gamma-ray energy spectrum of the central component in the entire energy range from 0.8 to 40 TeV is well described by a power law with an exponential cutoff, $I(> E_\gamma) = (2.92 \pm 0.11) \times 10^{-13} \times E_\gamma^{-1.55 \pm 0.10} \times \exp(-E_\gamma/10 \text{ TeV}) \text{ cm}^{-2} \text{ s}^{-1}$. (see Fig. 11, the black triangles). When the source's spectrum in the energy range 0.8 – 20 TeV is described by a simple power law $F(E_0 > 0.8 \text{ TeV}) \propto E^{k_\gamma}$, the spectral index is $k_\gamma = -1.92 \pm 0.11$. The SHALON spectrum corresponding to the emission from the central

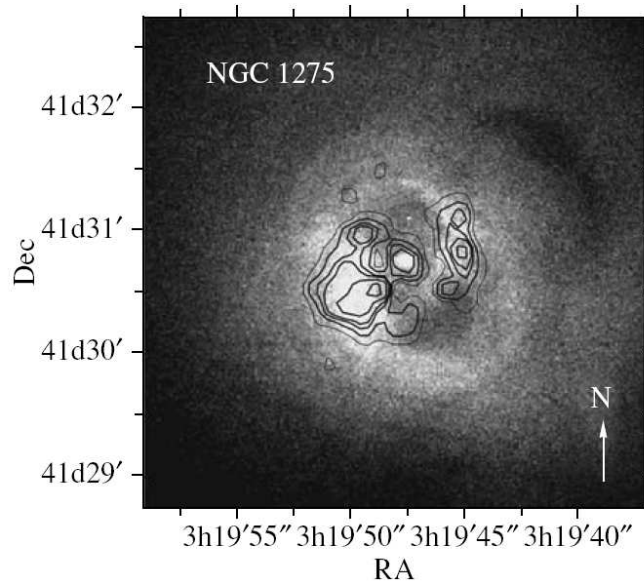


FIG. 10: Chandra X-ray (1.5 - 3.5 keV) image of NGC 1275 (Fabian et al. 2000); the contours indicate the SHALON image of NGC 1275 in the energy range 800 GeV - 40 TeV.

region of NGC 1275 is represented in Fig. 11 by the black triangles.

Recently, the AGN NGC 1275 was also recorded by the MAGIC ground-based mirror Cherenkov telescope at energies above 100 GeV in the 2010 - 2011 observations (Aléksic et al. 2012). Figure 11 compares the

integral gamma-ray spectrum of NGC1275 and its central region obtained from SHALON data (1996 - 2012) with the Fermi LAT (2009 - 2011) (Brown and Adams 2011) and MAGIC (2010 - 2011) (Aléksic et al. 2012) experimental data.

VARIABILITY OF THE GAMMA-RAY EMISSION FROM NGC 1275

Reliably revealing flares and their duration in long-term observations with mirror Cherenkov telescopes is complicated by the fact that the technique makes a continuous tracking of the source impossible, because it requires such conditions as moonless nights, which already creates a gap in the data for more than ten days; an ideal atmosphere without clouds and haze and, in addition, the source's passage at a distance of no more than 35° from zenith are needed, because the influence of a change in atmospheric thickness should be minimal.

Nevertheless, revealing correlations between the emissions in different energy ranges, comparing the emission regions, and, in particular, the detection of the flux changes remains necessary, because it makes it possible to judge the nature of the source, its evolution, and the emission generation mechanisms in various objects.

The observed gamma-ray flux variations, on average, do not exceed 20% of $(7.8 \pm 0.5) \times 10^{-13} \text{ cm}^{-2} \text{ s}^{-1}$. The SHALON mirror Cherenkov telescope has detected three short-time (within five days) increases and one decrease of the very high energy gamma-ray flux in the entire time of observations of NGC 1275. Given these variations, the flux decrease below the average was recorded in 1999

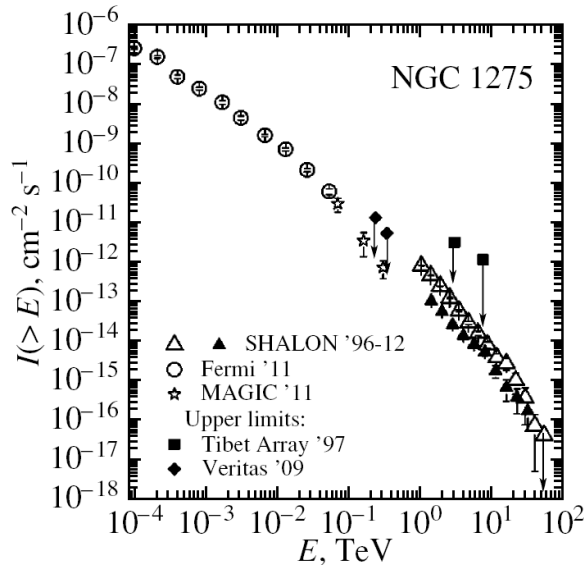


FIG. 11: Integral spectrum of high and very high energy gamma rays from NGC 1275 obtained by SHALON in comparison with the data from the Fermi LAT satellite telescope, the MAGIC and VERITAS mirror Cherenkov telescopes, and the scintillation Tibet Array.

and the integral flux was $(4.7 \pm 1.3) \times 10^{-13} \text{ cm}^{-2} \text{ s}^{-1}$. The increases were detected in late January 2001, late November-early December 2005, and late October 2009. The fluxes in these periods were $(21.2 \pm 7.5) \times 10^{-13}$, $(35.5 \pm 12.4) \times 10^{-13}$, and $(23.4 \pm 4.5) \times 10^{-13} \text{ cm}^{-2} \text{ s}^{-1}$, respectively. The duration of the flux increase in October 2009 was 3 days. No intervals of flux increase were found in 2001 and 2005, because the observations were interrupted due to weather conditions in both cases.

To reveal possible correlations of the emissions in various energy ranges, including those at high and very high energies, we compared the NGC 1275 gamma-ray fluxes by SHALON in the periods when the observations were simultaneous with the ones by the Fermi LAT experiment. The published Fermi LAT data were obtained from August 4, 2008, to September 30, 2010 (Brown and Adams 2011). The SHALON observations of NGC 1275 were performed in November 2008 with a break for the Moon's time, October 2009, and mid-November-early December 2010. In this time, only one gamma-ray flux increase to $(23.4 \pm 4.5) \times 10^{-13} \text{ cm}^{-2} \text{ s}^{-1}$ was detected in the period of October 18 - 20, 2009. These periods of SHALON observations do not coincide with the times of the main flares observed at Fermi LAT (Brown and Adams 2011). A slight local flux increase can be seen in the period of mid-October 2009 (Brown and Adams 2011), which corresponds to the above-mentioned gamma-ray flux increase observed by SHALON.

NGC 1275 AS A POINT AND EXTENDED SOURCE

As has been pointed out above, the Perseus cluster of galaxies with the central galaxy NGC 1275 is ideally suitable both for studying the physics of relativistic jets from AGNs and for revealing the feedback role of the central galaxy. Evidence for the latter was obtained in ROSAT and Chandra observations at low energies, from which shells of hot gas and cavities that spatially coincide with the radio structures originating in the central, active part of the AGN can be seen (Fig. 1 and Böhringer et al. 1993; Fabian et al. 2000, 2006; Churazov et al. 2000). The observational data for NGC 1275 at energies 800 GeV - 40 TeV, namely the images of the galaxy and its surroundings (Figs. 9 and 10), as well as the flux variations suggest that the TeV gamma-ray emission in these regions is produced by a number of processes.

The extended structure around NGC 1275 (Fig. 9) that spatially coincides with the X-ray emission regions (Fig. 10) can be produced by mechanisms related to the generation of an X-ray structure (Fabian et al. 2000, 2006; Churazov et al. 2000). The brightness distribution of the X-ray emission and the observed TeV emission shows a sharp increase in intensity immediately outside the bubbles blown by the central black hole and visible in the radio band. This suggests that the X-ray-generating particles are swept up from the region of the radio lobes

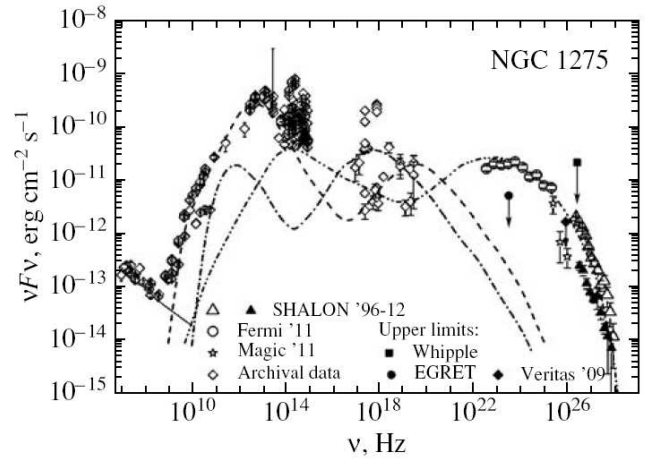


FIG. 12: Spectral energy distribution of the gamma-ray emission from NGC 1275. \triangle , \blacktriangle – represent the data from the SHALON ground-based Cherenkov telescope. \circ – represent the Fermi LAT and Magic data. The arrows indicate the upper limits from EGRET, Whipple, and VERITAS data (see the text). The dashed, dashdotted, and dashdotted with two dots curves indicate the spectral energy distributions of NGC1275 obtained in the CM model (Colafrancesco et al. 2010).

under the pressure of cosmic rays and magnetic fields generated in the jets at the center of NGC 1275 (Fabian et al. 2006; Churazov et al. 2000). The structures visible in TeV gamma rays are formed through the interaction of very high energy cosmic rays with the gas inside the Perseus cluster and interstellar gas heating at the boundary of the bubbles blown by the central black hole in NGC 1275.

The presence of emission in the energy range 1C40 TeV from a central region of $\sim 32''$ in size around the nucleus of NGC 1275 (see Fig. 11, the black triangles) and the short-time flux variability point to the origin of the very high energy emission as a result of the generation of jets ejected by the central supermassive black hole of NGC 1275. The multifrequency spectral energy distribution for the nucleus of NGC 1275, up to high and very high energies, was described in the CM model (Colafrancesco et al. 2010) and is a composition of the components of inverse Compton scattering of the intrinsic synchrotron radiation from relativistic electrons (synchrotron self-Compton) of three separate plasma blobs ejected from the inner regions of the NGC 1275 nucleus (Fig. 12, the dashed, dash dotted, and dashdotted with two dots curves). The available Fermi LAT data at high energies and the SHALON observations at very high energies in a region $< 32''$ around NGC1275 are described in terms of this model with one of the components produce synchrotron self-Compton emission of the relativistic jets from the nucleus itself (Fig. 12, the dashdotted with two dots curve).

CONCLUSION

The cluster of galaxies in Perseus, along with other clusters, have long been considered as possible candidates for the sources of high and very high energy gamma-ray emission generated by various mechanisms. Long-term studies of the central galaxy in the cluster, NGC 1275, are being carried out in the SHALON experiment. We presented the results of fifteen-year-long observations of the AGN NGC 1275 at energies 800 GeV - 40 TeV discovered by the SHALON telescope in 1996 (SinitSYna 1997, 2000; SinitSYna et al. 1998, 2003, 2006, 2007, 2009; Nikolsky and SinitSYna 2004). The data obtained at very high energies, namely the images of the galaxy and its surroundings, and the flux variability indicate that the TeV gamma-ray emission is generated by a number of processes: in particular, part of this emission is generated by relativistic jets in the nucleus of NGC 1275 itself. Whereas, the presence of an extended structure around NGC 1275 is evidence of the interaction of cosmic rays and magnetic fields generated in the jets at the galactic center with the gas of the Perseus cluster.

APPENDIX

Figure 13 presents the distribution in Θ^2 for the signal (*on*) and background (*off*) events recorded during the observations of NGC 1275 in the SHALON experiment

in 271.2 h. Θ^2 is the distance between the sources position and the shower direction to the source reconstructed in the experiment. The observed excess corresponds to 31.4σ determined according to Li and Ma (1983).

The table gives the signal excess above the background for each energy interval of the differential spectrum, the signal detection confidence level according to Li and Ma (1983) in each interval, and the differential flux. The differential spectrum of NGC 1275 is presented in Fig. 14.

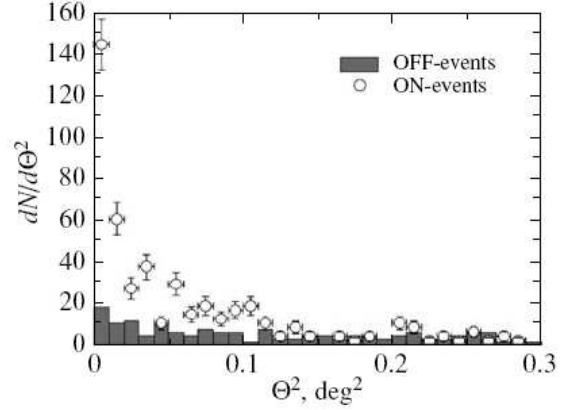


FIG. 13: Distribution of Θ^2 for the *on* and *off* events recorded in the SHALON observations of NGC 1275.

Flux measurements in each energy interval

| E, TeV | Excess | σ , (Li&Ma) | dF/dE , $\text{cm}^{-2}\text{s}^{-1}\text{TeV}^{-1}$ |
|--------|--------|-----------------------|---|
| 0,904 | 39 | 8,3 | $(9,59 \pm 1,53) \times 10^{-13}$ |
| 1,22 | 54 | 10,6 | $(4,45 \pm 0,60) \times 10^{-13}$ |
| 1,66 | 41 | 8,9 | $(1,39 \pm 0,22) \times 10^{-13}$ |
| 2,25 | 47 | 9,8 | $(7,52 \pm 1,01) \times 10^{-14}$ |
| 3,05 | 64 | 14,5 | $(5,26 \pm 0,65) \times 10^{-14}$ |
| 4,13 | 34 | 10,3 | $(1,51 \pm 0,26) \times 10^{-14}$ |
| 5,60 | 19 | 8,2 | $(4,76 \pm 0,91) \times 10^{-15}$ |
| 7,59 | 18 | 8,1 | $(2,63 \pm 0,62) \times 10^{-15}$ |
| 10,2 | 6 | 4,3 | $(4,44 \pm 1,98) \times 10^{-16}$ |
| 13,9 | 10 | 5,9 | $(4,83 \pm 1,61) \times 10^{-16}$ |
| 18,9 | 5 | 4,0 | $(1,32 \pm 6,62) \times 10^{-16}$ |
| 25,6 | 4 | 3,8 | $(6,27 \pm 3,62) \times 10^{-17}$ |
| 34,7 | 2 | 2,7 | $(2,47 \pm 1,75) \times 10^{-17}$ |
| 47,0 | 1 | 1,5 | $(1,75 \pm 1,00) \times 10^{-17}$ |

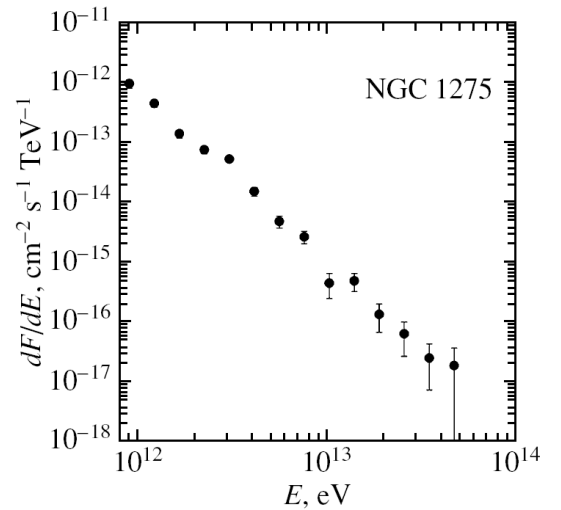


FIG. 14: Differential spectrum of NGC 1275 from SHALON data.

-
- [1] A. A. Abdo, M. Ackermann, M. Ajello, et al., *Astrophys. J.* **699**, 31 (2009).
- [2] V. A. Acciari, E. Aliu, T. Arlen, et al., *Astrophys. J.* **706**, L275 (2009).
- [3] J. Aléksic, L. A. Antonelli, P. Antoranz, et al., *Astrophys. J.* **710**, 634A (2010).
- [4] J. Aléksic, E. A. Alvarez, L. A. Antonelli, et al., *Astron. Astrophys.* **539**, L2 (2012).
- [5] M. Amenomori, in *Proceedings of the 26th International Cosmic Ray Conference*, Ed. by D. Kieda, M. Salamon, and B. Dingus (Salt Lake City, 1999), Vol. 3, p. 418.
- [6] J. R. P. Angel and H. S. Stockman, *Ann. Rev. Astron. Astrophys.* **18**, 321 (1980).
- [7] K. Asada, S. Kamenoi, Z.-Q. Shen, et al., *Publ. Astron. Soc. Jpn.* **58**, 261 (2006).
- [8] K. Asada, S. Kamenoi, Z.-Q. Shen, H. Shinji, D. C. Gabuzda, and M. Inoue, *Astron. Soc. Pacif. Conf.* **402**, 91A (2009).
- [9] H. Böhringer, W. Voges, A. C. Fabian, et al., *Mon. Not. R. Astron. Soc.* **264**, L25 (1993).
- [10] A. M. Brown and J. Adams, *Mon. Not. R. Astron. Soc.* **413**, 2785 (2011).
- [11] E. Churazov, W. Forman, C. Jones, and H. Böhringer, *Astron. Astrophys.* **356**, 788 (2000).
- [12] S. Colafrancesco and P. Blasi, *Astropart. Phys.* **9**, 227 (1998).
- [13] S. Colafrancesco and P. Marchegiani, *Astron. Astrophys.* **502**, 711 (2009).
- [14] S. Colafrancesco, P. Marchegiani and P. Giommi, *Astron. Astrophys.* **519**, A82 (2010).
- [15] B. Dennison, *Astrophys. J.* **239**, L93 (1980).
- [16] A. C. Fabian, E.M.Hu, L. L. Cowie, et al., *Astrophys. J.* **248**, 47 (1981).
- [17] A. C. Fabian, J. S. Sanders, S. W. Allen, et al., *Mon. Not. R. Astron. Soc.* **318**, L65 (2000).
- [18] A. C. Fabian, J. S. Sanders, G. B. Taylor, et al., *Mon. Not. R. Astron. Soc.* **366**, 417 (2006).
- [19] B. L. Fanaroff and J. M. Riley, *Mon. Not. R. Astron. Soc.* **167**, 31P (1974).
- [20] J. S. Gallagher, *Astron. Nachr.* **220**, 1040G (2009).
- [21] A. V. Goncharukii, A. M. Cherepashchuk, and A. G. Yagola, *Ill-Posed Problems in Astrophysics* (Nauka, Fizmatlit, Moscow, 1985) [in Russian].
- [22] A. M. Hillas, in *Proceedings of the 19th International Cosmic Ray Conference*, La Jolla, USA (NASA, Goddard Space Flight Center, 1985), Vol. 3, p. 445.
- [23] B. P. Houston, A.W.Wolfendale, and E. C.M. Young, *J. Phys. G: Nucl. Phys.* **10**, L147 (1984).
- [24] P. Kharb, M. L. Lister, N. J. Cooper, et al., *Astrophys. J.* **710**, 764K (2010).
- [25] T.-P. Li and Y.-Q. Ma, *Astrophys. J.* **272**, 317 (1983).
- [26] F. K. Liu and X. Chen, *Astrophys. J.* **671**, 1272 (2007).
- [27] F. Miniati, T. W. Jones, H. Kang, et al., *Astrophys. J.* **62**, 233 (2001).
- [28] S. I. Nikolsky and V. G. Sinitsyna, in *Proceedings of the International Workshop of Very High Energy Gamma-Ray Astronomy*, Ed. by A. A. Stepanian, D. J. Fegan, and W. F. Cawley (Crimea, 1989), p. 11.
- [29] S. I. Nikolsky and V.G. Sinitsyna, *Phys. At. Nucl.* **67**, 1900 (2004).
- [30] J. S. Perkins, H. M. Badran, G. Blaylock, et al., *Astrophys. J.* **644**, 148 (2006).
- [31] C. L. Sarazin, *Astrophys. J.* **520**, 529 (1999).
- [32] V. G. Sinitsyna and V. Yu. Sinitsyna, *Kratk. Soobshch. Fiz.* **4**, 1 (2011a).
- [33] V. G. Sinitsyna and V. Yu. Sinitsyna, *Astron. Lett.* **37(9)**, 621 (2011b).
- [34] V. G. Sinitsyna, in *Proceedings of the Workshop, Towards aMajor Atmospheric CherenkovDetector IV*, Ed. by M. Cresti (Univ. of Padova, Padova, 1995), p. 133.
- [35] V. G. Sinitsyna, *Nuovo Cim.* **19C**, 965 (1996).
- [36] V. G. Sinitsyna, in *Proceedings of the Workshop, Towards aMajor Atmospheric Cherenkov Detector V*, Kruger Park, South Africa, Ed. by O. De Jager (Westprint, Potchefstroom, 1997), p. 136.
- [37] V. G. Sinitsyna, *AIP Conf. Proc.* **515**, 293 (2000).
- [38] V. G. Sinitsyna, *Rad. Phys. Chem.* **75**, 880 (2006).
- [39] V. G. Sinitsyna, F. I. Musin, S. I. Nikolsky, et al., *Nucl. Phys. B (Proc. Suppl.)* **196**, 442 (2009).
- [40] V. G. Sinitsyna, S. I. Nikolsky, V. Y. Sinitsyna, et al., *Nucl. Phys. B (Proc. Suppl.)* **75A**, 352 (1999).
- [41] V. G. Sinitsyna, S. I. Nikolsky, V. Y. Sinitsyna, et al., *Nucl. Phys. B (Proc. Suppl.)* **122**, 409 (2003).
- [42] V. G. Sinitsyna, S. I. Nikolsky, V. G. Sinitsyna, et al., *Bull. Russ. Acad. Sci.* **71**, 906 (2007).
- [43] M. Strauss, J. P. Huchra, M. Davis, et al., *Astrophys. J. Suppl. Ser.* **83**, 29S (1992).
- [44] A. W. Strong, G. F. Bignami, P. A. Caraveo, et al., *Astron. Astrophys.* **115**, 404 (1982).
- [45] G. B. Taylor and R. C. Vermeulen, *Astrophys. J.* **457**, L69 (1996).
- [46] D. J. Thompson, D. L. Bertsch, B. L. Dingus, et al., *Astrophys. J. Suppl.* **101**, 209 (1995).
- [47] A. N. Tikhonov and V. Ya. Arsenin, *Solutions of Ill-Posed Problems* (Nauka, Moscow, 1979; Halsted, New York, 1977).
- [48] A. N. Timokhin, F. A. Aharonian, and A. Yu. Neronov, *Astron. Astrophys.* **417**, 391 (2004).
- [49] C. M. Urry and P. Padovani, *Publ. Astron. Soc. Pacif.* **54**, 215 (1995).
- [50] R. C. Vermeulen, A. C. S. Readhead, and D. C. Backer, *Astrophys. J.* **430**, L41 (1994).
- [51] M. P. Veron-Cetty and P. Veron, *Quasars and Active Galactic Nuclei*, 8th ed., ESO Sci. Rep. No. 18 (ESO, 1998); ADC/CDS Catalogue No. 7207 (1998).
- [52] R. J. Wilman, A. C. Edge, and R. M. Johnstone, *Mon. Not. R. Astron. Soc.* **359**, 755 (2005).